Applicability of the Peclet number approach to blow-off and flashback limits of common steelworks process gases

A.P. Giles[*], R. Marsh, P.J. Bowen, A. Valera-Medina

Cardiff School of Engineering, Queen's Buildings, the Parade, Cardiff, Wales, UK, CF24 3AA
* Corresponding author. Email: gilesap1@cardiff.ac.uk; Tel/Fax. +44(0) 29 2087 5931

Abstract

The ever-increasing importance of energy efficiency has given rise to numerous areas of concern for operators and developers of combustion plants; as the need to utilise fuel gases of increasingly poor quality and variability is essential for sustainability, while emission standards continuing to become more stringent. Swirl combustors are ubiquitous in industry owing to their great stability range which occurs due to the formation of a CRZ, which through the recycling of heat and active chemical species to the root of the flame enhances stability over a wide range of operating conditions.

Alternative fuels containing hydrogen offer the possibility of reduced greenhouse gas emissions; however flashback is of special concern with hydrogen enriched fuels, owing to the very high flame speed of hydrogen. Many by-products of process and waste industries can include a high proportion of hydrogen, for example Coke Oven Gas. Alternatively, many by-product process gases can contain a high proportion of non-combustible species such as nitrogen and carbon dioxide which can substantially reduce their flame speed and as a consequence increase the possibility of the flame extinguishing through blow-off.

This paper examines the blow-off and flashback potential of common steelworks process gases (including one which contains hydrogen) in a compact, premixed swirl burner in swirl number regimes representative of those found in practical systems. Methane is used as a base fuel for comparison. All results are obtained at atmospheric pressure without air preheat.

The Peclet number modelling approach incorporating a flame quenching parameter was applied to the results obtained for each of the fuel gases. Using this model, the quench factor value was seen to be dependent on burner configuration as well as fuel composition.

It was found that the stable burner operating conditions significantly change from fuel to fuel; with the operating points at which flashback occurs with Coke Oven Gas producing blow-off with weaker process gases such as Blast Furnace Gas and Basic Oxygen Steelmaking gas.

Nomenclature

CRZ	Central Recirculation Zone	[-]	S	Swirl Number	[-]
G	Axial momentum flux	[kg/s]	S_g	Geometrical Swirl Number	[-]
h	Height of tangential inlets	[mm]	S_L	Laminar burning velocity	[m/s]
m_t	Mass flow air and fuel	[kg/s]	t	Tangential inlet width	[mm]
n	Number of tangential inlets	[-]	U	Mean burner exit velocity	[m/s]
Pe	Peclet Number	[-]	W	Mean azimuthal velocity	[m/s]
Re	Reynolds Number ($=\rho UD/\mu$)	[-]	α	Thermal diffusivity	[m^2/s]
r_o	Combustor exit radius ($=D/2$)	[mm]	ρ	Density	[kg/m^3]
r_i	Combustor inlet radius	[mm]	φ	Equivalence ratio	[-]
r_p	Fuel injector radius	[mm]	μ	Dynamic Viscosity	[kg/ms]

1. Introduction

There are a variety of energy intensive processes involved in the production of steel in a modern integrated steelworks, often involving the combustion of significant volumes of fuel gases, both indigenous and imported. During the coke making, iron making and steel conversion processes occurring within an integrated steelworks, energy rich by-product gases are generated which are utilised onsite to reduce the requirement for imported natural gas.

Coke Oven Gas (COG) is produced during the coking process, in which carbon-rich coke is produced by the pyrolytic heating of coal. COG primarily consists of hydrogen and methane, but also contains carbon monoxide, carbon dioxide, ethane, nitrogen and trace amounts of oxygen. During the iron making process coke (and other reductants) are used to chemically reduce iron ore in a blast furnace; in which preheated blast air reacts exothermically with the coke to produce carbon monoxide, some of which acts as a reducing agent for the iron ore to produce molten iron and carbon dioxide. The by-product Blast Furnace Gas (BFG) consists mainly of nitrogen, with carbon monoxide, carbon dioxide and a small proportion of hydrogen. The molten iron is converted into steel by reducing its carbon content using the Basic Oxygen Steelmaking (BOS) process, in which a lance is used to blow pure oxygen into the molten iron. The by-product of this process is BOS gas which is composed mainly of carbon monoxide with small proportions of carbon dioxide and nitrogen and a trace amount of hydrogen. However, there is a great deal of variability in the composition of the individual steelworks gases, with the hydrogen and methane content of COG being heavily dependent on the type of coal being used (the hydrogen and methane content typically being of the order of 39 - 65 % and 20- 42 % respectively [1]). Depending on the technology employed in the blast furnace operation, the carbon monoxide content of the BFG can vary between 20 and 28%; while the hydrogen content is typically between 1 and 5% [1]. The batch nature of the BOS gas production process results in the composition of the gas captured also varying, with the carbon monoxide content typically between 55 and 80% and hydrogen between 1 and 10% [1].

The dynamic nature of the processes producing these indigenous gases results in a constantly varying composition, which for the lower energy density BFG can significantly affect the fuel properties of the by-product gases, with the laminar burning velocity [2] and the water vapour content and particulate loading [3] varying both over time and transport distance from the furnace.

The efficient utilisation of the steelworks process gases can potentially reduce the need for importing natural gas, improving the overall energy demand per unit mass of steel produced and reducing CO_2 emissions. These three steelworks by-product gases, because of the difference in their compositions, have completely different flame characteristics and stability limits, of which there is comparatively little data available.

Work carried out by Paubel et al. [4] investigated the oxy-combustion stability of BFG, which showed that with a methane pilot and pure oxygen as an oxidant, the stability of combustion of the low caloric value BFG can be improved. Hou et al. [5] carried out a comparison of the flame properties of various BFG and COG combinations, highlighting the technical difficulty in combusting BFG without the use of a pilot or blending with a fuel of higher quality. However, the efficient combustion of process gases in modern industrial swirl burners and gas turbines requires a more detailed understanding of the blow-off and the flashback limits of the different fuels, and the effect that changes in combustor configuration has on these stability boundaries.

Swirl combustors are almost universally used within gas turbines along with many other combustion processes due to the benefit of increased mixing of the fuel and air along with increased flame stability and improved blow-off limits. The latter is extremely important for gas turbine operation and is affected by many characteristics, namely; fuel type, the geometry of the burner and hence its swirl number and the combustion process being used; diffusion, premixed or partially premixed [6, 7].

The swirl number (S) is the primary parameter used for the characterization of swirling flows, and is defined as the ratio of the axial flux of angular momentum (G_θ) divided by the axial flux of axial momentum (G_x), and the nozzle radius (r_0) [8, 9], as is given below in Equation 1:

(1) $\quad S_0 = {G_\theta}/{G_x r_o}$

A major effect of swirling flows is the presence of a centrally located recirculating flow, described by Valera-Medina et al [10 – 12], which is an important mechanism for energy exchange and the recycling of heat and active chemical species to the root of the flame when combustion is occurring. Under stable operating conditions the effect of combustion is an increase in the axial flux of axial momentum when compared to that of an isothermal flow (without combustion) for the same flow conditions; whilst scarcely affecting the axial flux of angular momentum

[13, 14]. As a result, for the same burner geometry, the flow with combustion will have a reduced swirl number and a decrease in the size and extent of the central recirculation zone (CRZ). For a generic swirl burner, in order to produce accurate computer simulations an understanding of how the operating conditions affect the three-dimensional velocity field and the CRZ location /size requires detailed measurements of the flow to be taken. The two parameters G_θ and G_x can be expanded [15], allowing Equation 1 to be rewritten as a radial integral involving terms for the burner exit and azimuthal velocities (U and W), density (ρ) and pressure (P):

$$(2) \quad S_0 = \left. \int_0^R (Wr)\rho U 2\pi r\, dr \middle/ r_o \left(\int_0^R 2\pi r\rho U^2\, dr + \int_0^R 2\pi r P\, dr \right) \right.$$

In practice however, as the flow patterns are highly complex, it is difficult to specify the exact experimental swirl number, unless very detailed static pressure measurements as well as 3D velocities are available, which for practical reasons is not common. It has been shown by Sheen et al [15] that by eliminating the pressure integral term in Equation 2, a good approximation can be obtained through the use of a modified swirl number (Equation 3), which only requires detailed velocity measurements for evaluation:

$$(3) \quad S = \left. \int_0^R UWr^2\, dr \middle/ r_o \int_0^R U^2 r\, dr \right.$$

A more common and simplified value of the swirl number is obtained from the geometric swirl number (S_g), which uses the geometry of the burner, hence requires the pressure variations across the flow to be neglected and the assumption of a constant density. Equation 4 defines the geometric swirl number of the system utilised in this study in relation to the dimensions of the burner tangential inlets and associated radii (which are described in table 1 and shown schematically and photographically in figures 1 & 2 respectively):

$$(4) \quad S_g = \left. \pi\left(r_o^2 - r_p^2\right)\left(r_i - {}^t/_2\right) \middle/ (n.t.h)r_o \right.$$

As can be seen from Equation 4, the geometric swirl number (S_g) is dependent only on the nozzle dimensions; with the flow operating conditions and pressures being ignored. The geometric swirl number allows the comparison of behaviour for burners of varying designs; as the use of different geometries and flow rates will produce a wide variation in densities and the adoption of a single non-dimensional number simplifies such results. It is clear, however, that the presence of combustion inherently alters the properties of the swirling flow and the formation of the coherent flow structures [16]. Therefore, any change in burner design or operating conditions can be seen to alter the size, strength and position of the CRZ, as well as its interaction with other flow structures and other secondary recirculation zones as observed in other studies [10].

Various parametric models have been used to represent the physical processes involved in combustion phenomena such as flashback and blow-off, with the Peclet Number approach being used to represent both flashback and blow-off conditions for a variety of burner configurations [17 – 19]. The Peclet Number approach utilises the fuel properties, equivalence ratio, flow velocity and burner geometry to represent the stability limits of a combustion system; with the flow Peclet Number having being shown to be proportional to the square of the flame Peclet Number [14].

$$(5) \quad Pe_{flow} \propto \left(Pe_{flame}\right)^2 \qquad \text{with}$$

$$(6) \quad Pe_{flow} = \frac{UD}{\alpha} \quad \text{and} \quad (7) \quad Pe_{flame} = \frac{S_L D}{\alpha},$$

Here U is the characteristic velocity (mean burner exit velocity), D is the characteristic dimension (burner exit diameter), S_L is the laminar burning velocity of the flame and α is the combustion mixtures thermal diffusivity. By adopting the flame quenching approach used by Kroner et al [14]; a quench parameter can be defined using the laminar flame speed, characteristic length scales, characteristic velocities and characteristic time scales. Flame quenching is said to occur at a critical value of this quench parameter such that:

$$(8) \quad C_{quench} \leq \frac{\alpha}{S_L^2} \cdot \frac{U}{D}$$

From this it can be seen that equation 5 can be modified further to show that:

$$(9) \quad \frac{UD}{\alpha} \sim C_{quench}\left(\frac{S_L D}{\alpha}\right)^2$$

Dam et al [19] found that the value of C_{quench} was found to be dependent on fuel composition and remained constant across different burner geometries. However, only small changes in fuel composition were investigated in that study. The aim of this present study is to investigate the flame stability limits of selected industrial fuel gases and to appraise the applicability of the Peclet number flame quenching modelling approach, identifying the effect of variations in fuel composition and burner configuration on the ability of the model to predict the stable operating limits.

2. Experimental Procedure

A swirl burner has been developed and used in previous studies [20 – 23] to investigate the flashback and blow-off behaviour of fuels with varying hydrogen content. This burner system has been designed to incorporate the aerodynamic features common with industrial and gas turbine combustors including variable swirl and confinement attachments; and its internal geometry can be varied through the use of different inserts (Details of the generic swirl burner system is shown in Fig. 1).
The burner system is of stainless steel construction and consists of a main body with a single main tangential inlet feeding an outer plenum chamber. Slot type radial tangential inlets are used to pass the unburned fuel and air into the burner, the fuel and air mixture then passes through the burner exhaust where the gases interact with the flame stabilizing central recirculation zone (CRZ). The exhaust nozzle length is equal to one exit radius as this has been shown by Valera-Medina et al. [24] to improve burner performance. Several swirl inserts are available, and are secured in the burner with a large outer housing; there is also the option to use a centrally located injector or secondary fuel / air nozzle. Details of the geometry of the swirl inserts and the dimensions used for this study are shown in Table 1 and Fig. 2.

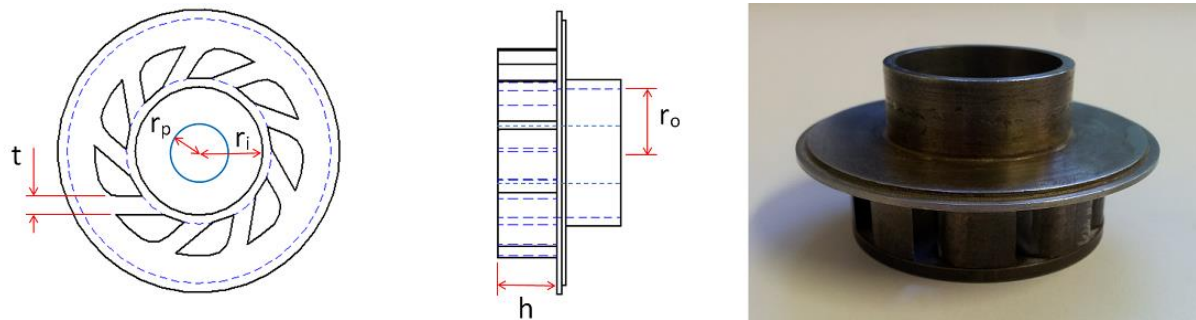**Fig. 1 a - Swirl burner assembly drawing, b - Image of assembled burner**

Fig. 2 a - Swirl burner-inlet configuration, b - Swirl insert of S_g=1.04

Table 1 Swirl Burner Dimensions

Swirl Condition	Swirl number (S_g)	Injector radius (r_p)	Inlet radius (r_i)	Exit radius (r_o)	Tangential inlets No. (n)	width (t)	Height of tangential inlets (h)
A	0.81	6.35mm	16mm	14mm	9	5mm	13mm
B	1.04	6.35mm	16mm	14mm	9	4mm	13mm
C	1.21	6.35mm	16mm	14mm	6	5mm	13mm
D	1.56	6.35mm	16mm	14mm	6	4mm	13mm

For swirl conditions A and B, it can be seen from table 1 that the burner geometry consisted of 9 tangential inlets to the burner exit chamber, for swirl conditions C and D the burner geometry consists of only 6 tangential inlets. The mass flow rates of both air and fuel were measured using suitably sized 'Micromotion' coriolis mass flow meters, which have an accuracy of ± 0.35% FS [25]. The equivalence ratios for the air/fuel mixture are calculated in terms of mass flow, which has a combined uncertainty of measurement of ± 0.48%. In addition, single point error bars representing 1 standard deviation are included on each of the experimental figures based upon a review of the overall experimental accuracy. The exact mass flow rates of the air and fuel at the blow-off condition was determined at a variety of flow conditions, with the burner being relit and the blow-off event repeated before recording the result. In order to improve confidence when determining the flow conditions at which flashback occurred, a thermal imaging camera was used to monitor the burner nozzle temperature and flame location. A flashback event was recorded if the flame position retreated into the burner exit causing an increase in burner temperature, before repeating each result the fuel flow was shut-off and the burner was allowed to cool down to ambient temperature conditions. Figure 3 shows thermal images of the burner apparatus at stable operating conditions before a flashback event occurs and immediately after a flashback event for both COG and methane fuels.
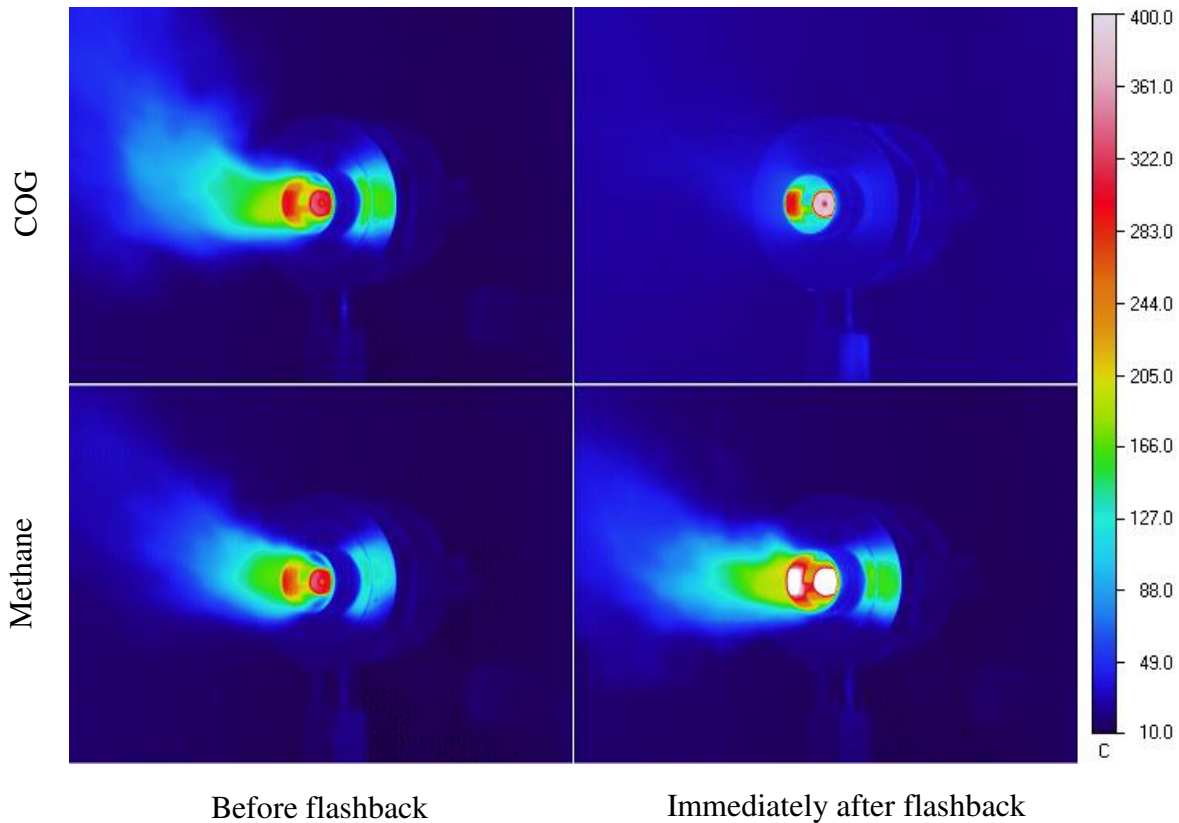

Before flashback   Immediately after flashback

Fig. 3 - Thermal images of flashback event for methane and COG (S_g=1.04)

The time difference between the 'before' and 'after' flashback images shown in Fig. 3 was approximately 1 second for both fuels, with a small reduction in air flow being the event which triggered the flashback in both cases. The approximate power (based on fuel flow rate and lower heating value) for both fuels in the cases shown was 2 kW. It can be seen from Fig. 3 that the flashback event is, broadly speaking, different for COG and Methane. From reviewing the videos taken of the flashback events during the experiments, the precise mechanism by which the flashback occurred for the COG could not be determined; as a small change in equivalence ratio and the comparatively fast burning rate of the fuel caused the flame to rapidly and completely retreat within the burner housing. For the methane fuel, for the particular burner configuration used during this work, it was possible to maintain the flame location at the burner exit at the flashback flow conditions. An examination of the videos taken of the methane flashback events showed that there was still evidence of a strong boundary layer structure at the flashback flow conditions, suggesting that mechanism by which flashback was occurring was Combustion Induced Vortex Breakdown, as described by Kröner et al [14] and Dam et al [19].

Four fuel blends were examined for each of the geometric swirl configurations; with the fuels studied being synthesised versions of the three steelworks by-product gases and methane as a benchmark. For methane as well as representative synthesised BFG and BOS gas [1], a cylindrical exhaust confinement with an internal diameter of 42 mm was fitted to the original 'unconfined' design, in order to examine its effect on the blow-off behaviour of the swirl burner for these gases in conditions more representative of gas turbines. The compositional details as well as selected properties of the four fuels studied are listed in Table 2, for the COG fuel the highest typical composition of hydrogen [1] was chosen as this would represent the worst case for flame stability. The stoichiometric laminar burning velocities for the fuels are predicted by Chemkin using the Gri-mech mechanism [26] for calculations with COG and methane, and the Li et al [27] mechanism for the BOS and BFG compositions.

Table 2 - Composition and properties of fuels studied

| Fuel	Composition by Volume	Fuel density (kg/m^3)	Fuel Gross CV (MJ/m^3)	Stoichiometric Laminar Burning Velocity (cm/s)	Stoichiometric AFR by mass
1 - Methane	100% CH_4	0.667	37.04	39.6	17.13
2 - Synthesized COG	65% H_2, 25% CH_4, 6% CO_2, 4% N_2	0.378	16.97	84.1	12.48
3 - Synthesized BFG	50% N_2, 23% CO_2, 22% CO, 5% H_2	1.264	3.18	5.6	0.61
4 - Synthesized BOS gas	65.3% CO, 19.3% N_2, 14.4% CO_2, 1% H_2	1.250	7.81	19.3	1.52

3.   Results

Fig. 4 displays the total mass flow at the blow-off condition with a burner S_g of 1.04 for all the fuels utilised. It can be seen that the total mass flow through the burner at the blow-off condition was much higher for the COG, with its 65% hydrogen content, than the rest of the fuels; with stable flames possible with COG at leaner operating conditions. The total mass flow at the blow-off limit for BOS gas, with 65% carbon monoxide and 1 % hydrogen, were found to be similar to that of methane over a range of operating conditions. However both BOS gas and methane were found to have higher blow-off limits than that of BFG, with BFG having the lowest total mass flow at blow-off conditions over all the equivalence ratios used in the experiments; which is explained by its lower burning velocity due to it containing 73% non-combustible content by volume.

The total mass flow at the flashback conditions for a S_g of 1.04 for the Methane and COG fuels are shown in Fig. 5. For the BFG and BOS gas fuels it was found during experimentation that not possible to obtain flashback data for BOS gas and BFG, as on the reduction of air mass flow for a given fuel flow the flame would transition through to either a weak diffusion flame or to a rich extinction, possibly due to the comparatively low burning rate of these fuels affecting the resulting flame location during transition. It can be seen that the total mass flow at which flashback can occur for COG is much higher than that of methane, with COG flames still able to produce flashback events at very lean burner operating conditions. Comparing the total burner mass flows for the COG flashback operating conditions shown in Fig. 5 to the blow-off limits of the BOS gas, BFG and methane shown in Fig. 4 it can be seen that COG will flashback at total mass flows higher than that of the blow-off conditions of the other three fuels.
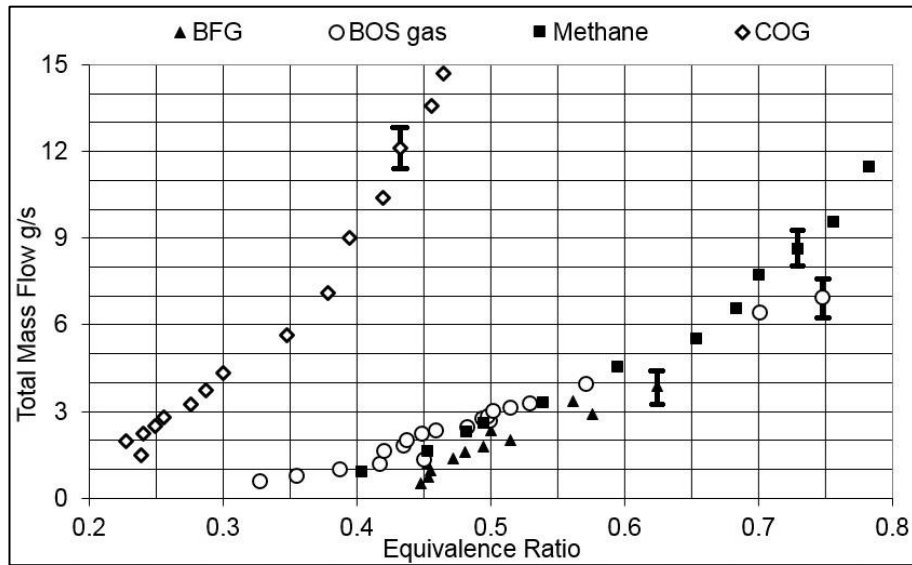
Fig. 4 - Total mass flow at blow-off limits for each of the fuels utilised, burner S_g=1.04.
For clarity, the stable operating condition is below the locus of points under consideration, and the blown-off (extinguished) condition is above.
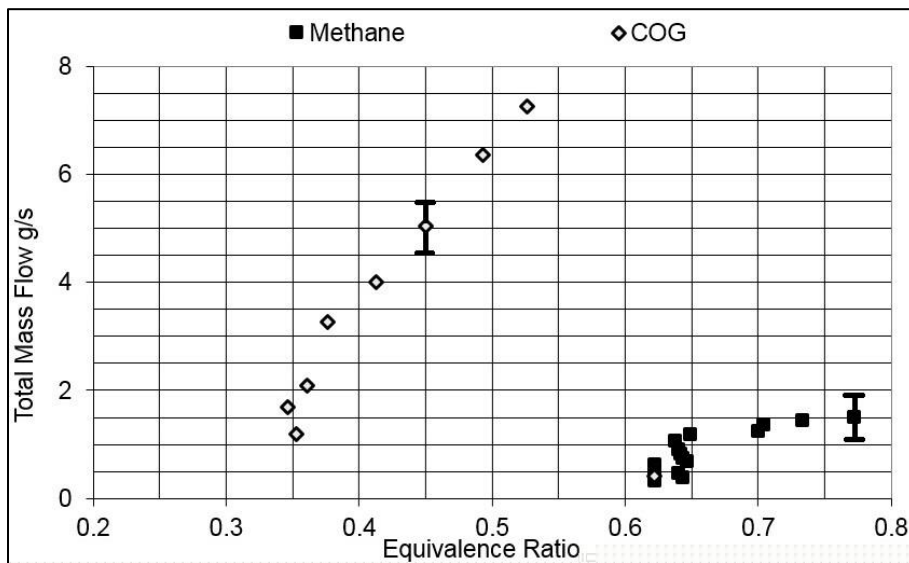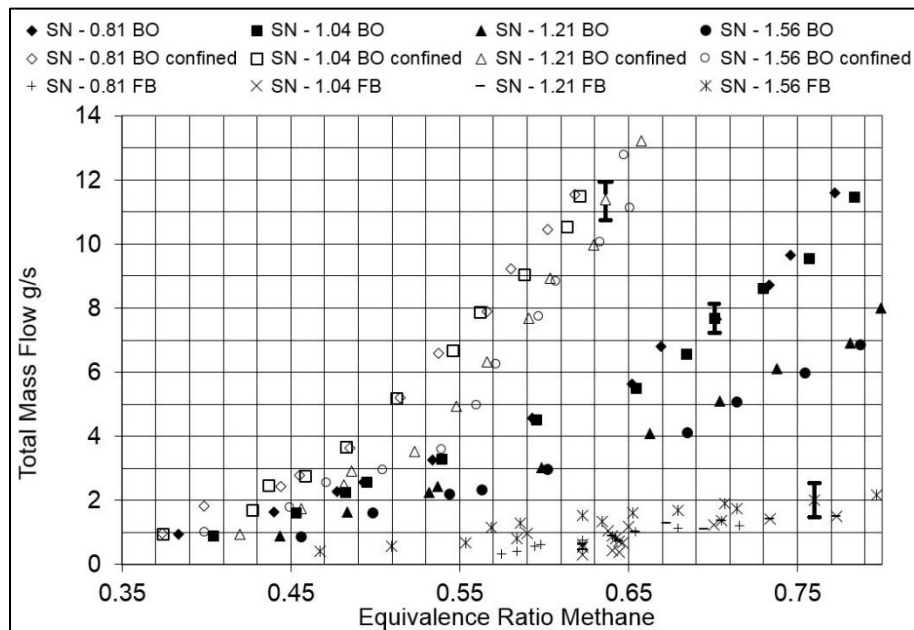

Fig. 5 - Total mass flow at flashback limits for COG and methane, S_g=1.04.
For clarity, the stable operating condition is to the left of the locus of points under consideration, and the flashback condition is right.

Looking at each of the fuels studied individually – beginning first with the results obtained for methane. Fig. 6 displays the total mass flow at the blow-off and flashback limits for methane for the four different swirl inserts used. It can be seen that for the range of swirl numbers utilised the total mass flow at the flashback limit are similar, with the highest mass flow at flashback seen with a swirl number of 1.56. A general trend can be seen in which the mass flow at flashback reduces as the swirl number is reduced but this is not conclusive. The effect of swirl number on flash back limits corresponds with that shown by Syred et al. [20] and Abdulsada et al. [21 – 23]. It can be seen that the total mass flow at the blow-off limit increases as the swirl number reduces, which is likely to be due to the lower

local velocities and therefore increased residence time having a larger effect on the Damköhler Number than that of the reduced turbulence levels and therefore lower turbulent flame speed. The use of confinement is shown to improve the blow-off limits for all the swirl inserts, with the total mass flow at the blow off limits for lower swirl numbers again being higher than that for the high swirl numbers. This agrees with that previously described by Valera-Medina et al [24], who concluded that the use of confinement prevents further dilution of the lean premixed flames by stopping air entrainment and improving flame stability.

It can be seen from Fig.6 that the small increase in total mass flow at the blow-off condition as the swirl number is reduced from 1.56 to 1.21 and from 1.04 to 0.81 is small compared when compared to the mass flow increase seen when the swirl number is reduced from 1.21 to 1.04. The dimensions used for each of the swirl configurations listed in Table 1 reveal that the 1.21 and 1.56 swirl configurations utilised 6 tangential inlets, whereas 9 tangential inlets are used in the 0.81 and 1.04 swirl numbers. Therefore the change in inlet number configuration is seen to have a much larger effect on the stability limits than the calculated change in geometric swirl number (Equation 4). This may be due in part to the different combustor configurations having different pressure characteristics; which is shown in Equation 2 to have an effect on the swirl number of the combustor, but is ignored in calculating the geometric swirl number.

Fig. 6 – Total mass flow at blow-off and flashback limits for methane, S_g=0.81 – 1.56

The unconfined blow-off and flashback limits for COG are shown in Fig. 7. Note how the total mass flow rate at blow-off is always higher than that for methane shown in Fig. 6, which is logical given the COG mixtures' higher flame speed. It can be seen that for the COG fuel, at the lowest equivalence ratios the stable operating regime between the blow-off and flashback limits is comparatively narrow, with only a small range of equivalence ratios in which a stable flame can be sustained. As the equivalence ratio is increased the area for stable operation widens; this phenomena was also seen by Syred et al. [20], Abdulsada et al. [21 – 23] and Shelil et al. [28]. As with methane, it can be seen that the blow-off limit improves as the swirl number is reduced. Examining the flashback results for COG shown in Fig. 7 it is seen that at very low mass flow rates there is a significant increase in the equivalence ratio at which flashback occurs; possible reasons for this will be discussed during the analysis section of this paper.
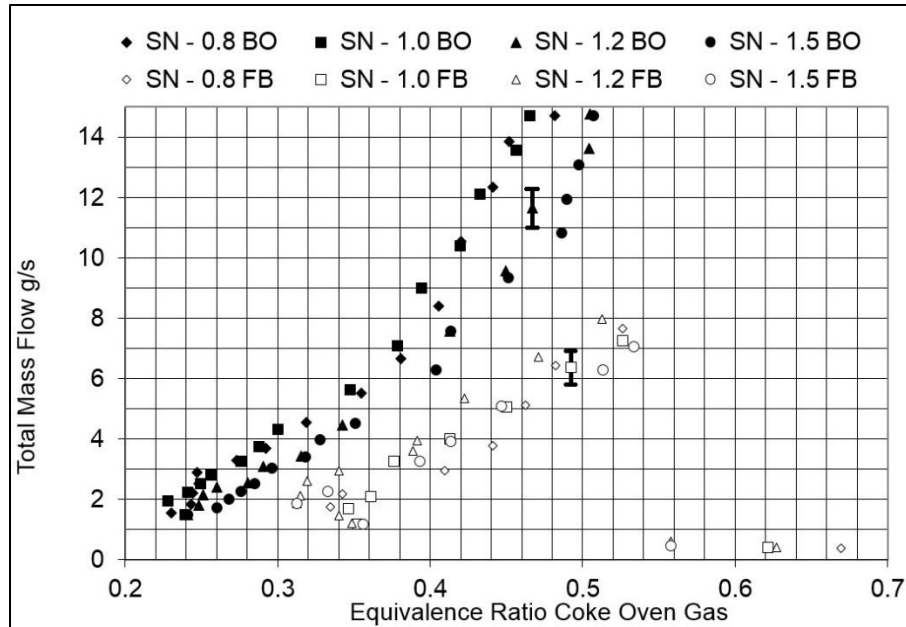
8

Fig. 7 – Total mass flow at blow-off and flashback limits for COG, S_g=0.81 – 1.56
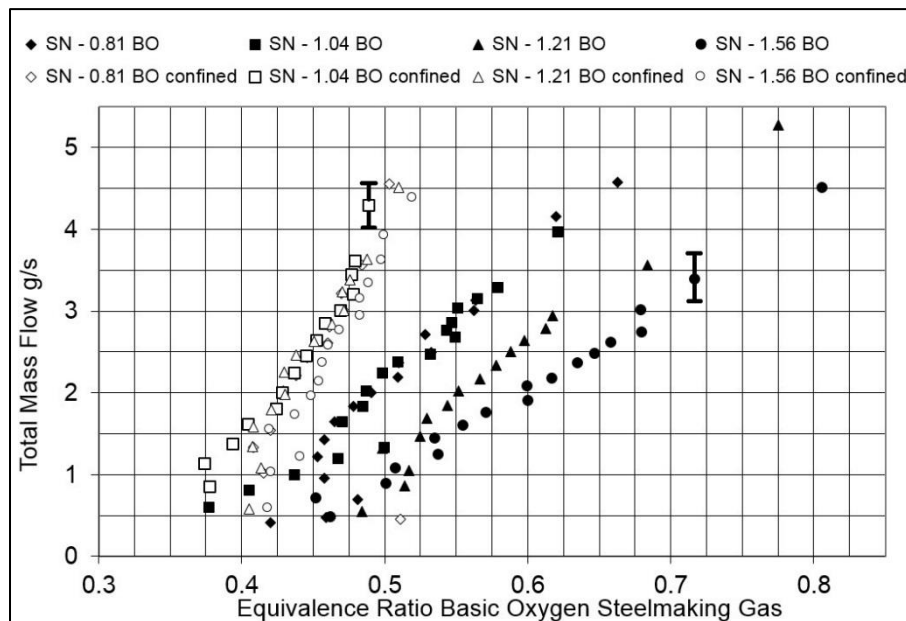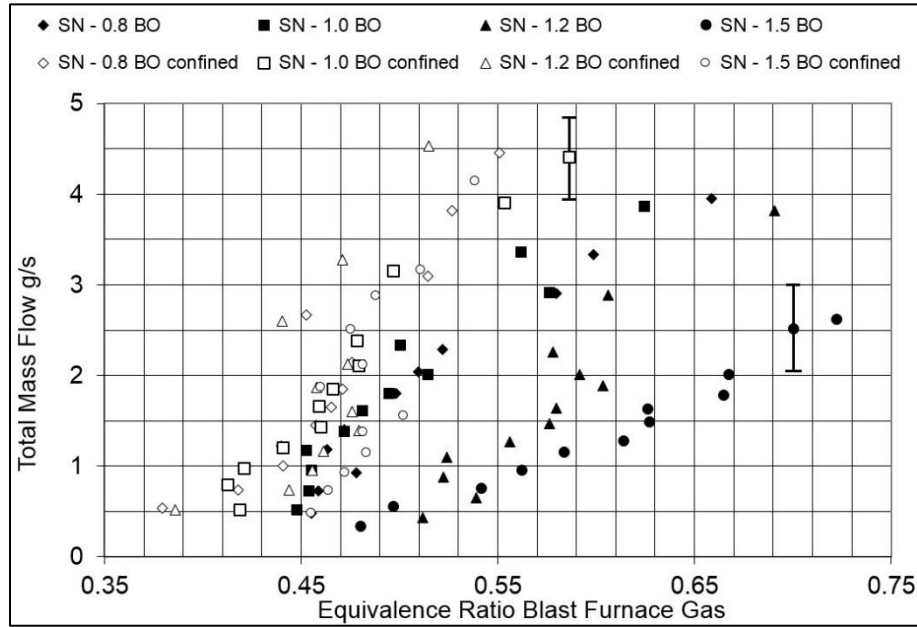

Fig. 8 – Total mass flow at blow-off limits for BOS gas, S_g=0.81 – 1.56

The total mass flow rate at the confined and unconfined blow-off limits for BOS gas and BFG are shown in Figs. 8 and 9 respectively. The unconfined blow-off limits for both BOS gas and BFG exhibit the same trend as that of the other fuels utilised; with lower swirl numbers having an increased total mass flow rate at the blow-off limit to that of high swirl numbers. The use of confinement is seen to improve the blow-off limit for both fuels, however it can be seen that compared to the results for Methane (Fig. 6) the effect of changing the swirl number on the blow off limit is reduced when confinement is used. This is likely to be because at the relatively low flow rates seen at the blow off limit for BOS gas and BFG, a substantially weaker CRZ is present for all swirl numbers used.

9

Compared to the data taken for the previous fuels, the results for BFG shown in Fig. 9 have a much greater variability; particularly when the total mass flow increases above approximately 2 g/s. This transition point may correspond to the flow exiting the combustor switching to being more turbulent, and the resultant increase in the flame speed of the fuel/air mixture.

Fig. 9 – Total mass flow at blow-off limits for BFG, S_g=0.81 – 1.56

4. Discussion and Analysis

There are clear trends evident when the blow-off and flashback results for the steelworks gases shown in Figs. 6 to 9 are compared; with the stable operation envelope being much narrower for the Coke Oven Gas (COG) than any of the other fuel gases utilised. For all of the fuels, the total mass flow at the blow-off limit was seen to increase with a reduction in burner swirl number; with the COG seen to be the most resistant to blow-off, requiring a much higher total mass flowrate for the flame to become detached from the burner. Of all the fuel gases used, the Blast Furnace Gas (BFG) was the most susceptible to becoming blown-off, while the Basic Oxygen Steelmaking (BOS) gas and methane fuel gases were found to require similar total mass flows to blow-off throughout the range of equivalence ratios utilised.

The flash back limits for methane and COG for the swirl numbers utilised are shown in Figs. 6 and 7. It can be seen from Fig. 6 that for methane the total mass flow at which flashback occurs is seen to increase as the burner swirl number increases. For COG, flashback is seen to occur with higher equivalence ratio values for the very low total mass flows. However, as the total mass flow is increased flashback occurs with COG at lower equivalence ratio values, reducing the stable operating envelope for this burner design to its narrowest at total mass flow values of between 2 and 3 g/s. As the total mass flow through the burner is further increased the equivalence ratio values at both the flashback and blow-off limits also increases, with the stable operating envelope widening with increased total mass flow.

In order to understand the trends shown in the results for the steelworks gases, an estimate of the Reynolds number of the flow through the burner exit at the blow-off and flashback limits was calculated for the gas/air mixture compositions. The viscosity of the gas mixtures at each of the flow conditions was calculated using the methods described by Wilke [29]. Fig. 10 displays the Reynolds number for Methane, COG BOS gas and BFG results for a swirl number of 1.04.

Examining the calculated values for the Reynolds numbers shown in Fig. 10, it can be seen that transition point previously identified in the COG flashback data occurs at a Reynolds number of approximately 4400 – highlighted.

This suggests that the change in behaviour observed in the COG flashback limit is due to a change in flow conditions. The flashback point with the lowest recorded mass flow occurs at an equivalence ratio of approximately 0.62, when according to Fig. 10 the flow is laminar in nature. As the mass flow is increased the equivalence ratio at flashback reduces as the flow changes to being turbulent at the transition point, with further increases in mass flow resulting in the equivalence ratio at flashback following a similar curve to that for the blow-off conditions. All of the methane flashback data points and some of the data points for the blow-off conditions for all fuels (particularly the BOS gas and BFG), are seen to have Reynolds number values representative of laminar flow conditions. As such it may be necessary to take this into account when further analysis is carried out.
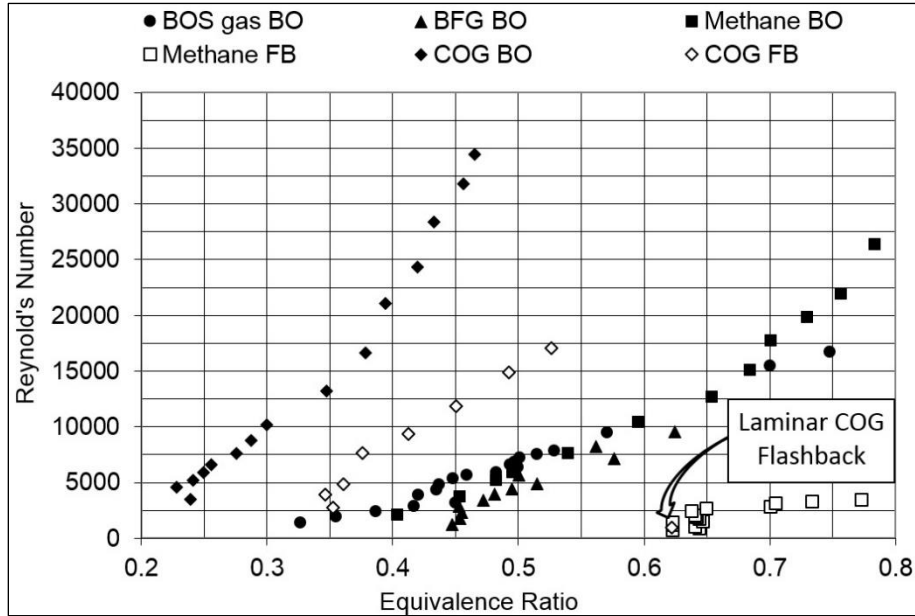

Fig. 10 – Calculated Reynolds number at blow-off / flashback limits for COG and methane, S_g=1.04.

In order to apply the Peclet number parametric modelling approach to the data obtained for the steelworks fuel gases, it is necessary to calculate values for the laminar burning velocity and thermal diffusivity of the fuel gas / air mixtures throughout the range of gas compositions used during experimentation.

Experimental data for the laminar burning velocity of the steelworks gas compositions has been obtained by Pugh et al [2, 30, 31] and the data relevant to the compositions used in this work is shown in Fig. 11. In addition, laminar burning velocities for the gas compositions used calculated using the Chemkin software are also shown in Fig. 11. For the BFG and BOS gas compositions, the Li et al [27] mechanism was utilised and is seen to have a good agreement with the experimental data, with the experimental data points overlaying that of the simulation results in Fig. 11. For the methane and COG gas compositions the Gri-mech mechanism [26] was used and is seen to be in good agreement with the experimental data for methane but to under-predict the laminar burning velocity of the COG fuel gas. Obtaining the laminar burning velocities of the gas compositions at lower equivalence ratios using the Chemkin software was found to be problematic, as during the simulation runs the software would be unable to converge upon a solution. In addition, experimentally derived laminar burning velocities were not available for the lower equivalence ratios, therefore extrapolated values of the laminar burning velocity were used when required. For the COG fuel, where there is a disagreement between the Chemkin and experimental data, the extrapolation uses the measured laminar burning velocity data.

To calculate the thermal diffusivity (α) of the gas compositions used during the experiments, the density of the gas mixtures was calculated based upon the molar fraction and density of the constituent molecules. The gas mixture thermal conductivity was calculated using the method described by Lindsay and Bromley [32], and the specific heat capacity of the gas mixture was found by summing the product of mass fraction and the specific heat capacity of the component species [33]. The Peclet numbers for the "flame" and "flow" for each of the data points obtained from the combustion experiments can then be obtained as defined in equations 6 and 7, using the calculated thermal diffusivity.

11
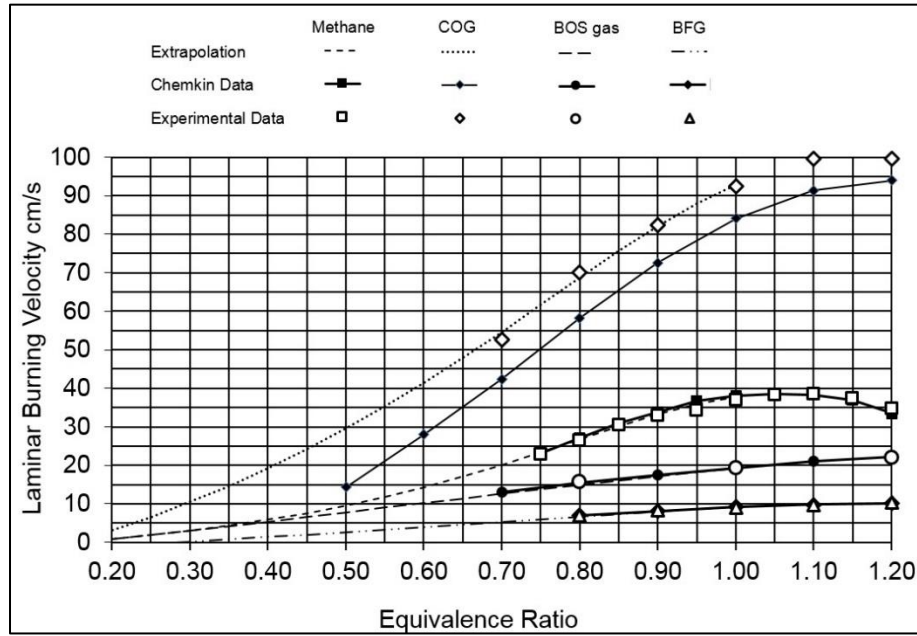
Fig. 11 –Laminar Burning Velocity of fuel gases utilised (Pugh et al. 2013, 2014, 2015)

Using equation 8, values for the C_{Quench} parameter can be obtained for each experimental result. In addition, equation 9 can be rearranged into the form:

$$(10)\log(Pe_{flame}) = \frac{1}{2}\log(Pe_{flow}) - \frac{1}{2}\log(C_{Quench})$$

Figs. 12 – 15 show the calculated values for C_{Quench} together with the correlation between the flow and laminar flame speed Peclet numbers for each of the fuel gases utilised in this study.

Fig. 12a presents the quenching relationship with methane as fuel for swirl numbers between 0.81 and 1.56. The data shows that across the range of swirl numbers utilised there is evidence that changing the burner configuration through increasing the swirl number can be seen to consistently cause a reduction in the calculated quench parameters for the blow-off conditions, both with and without confinement. The calculated quench parameters for the methane flashback conditions are seen to always be lower than that of the blow-off conditions, which is in turn lower than that of the blow-off conditions with confinement. The calculated quench parameter for the methane flashback data appears to only change slightly with swirl number, with an increase in the mean quench parameter value for the 1.56 swirl number when compared to that of the other swirl number values.

For Fig. 12b the average values for the quench parameter for the flashback, blow-off and confined blow-off conditions for methane (corresponding to 0.036, 0.192 and 0.449 respectively) were used to generate y-intercept values for trend lines. From the Peclet number results shown in Fig. 12b it can be seen that at higher swirl numbers there is a tendency for the flame to blow off at slightly higher S_L values (at constant U), which is attributed to a lower axial velocity of the flame, given the effects of the higher swirl component (and the resultant increase in turbulence). It can also be seen that for the flash back and the blow-off behaviour, the results for methane correlate reasonably well with equation 10, confirming the results of Kroner et al. [14].

12
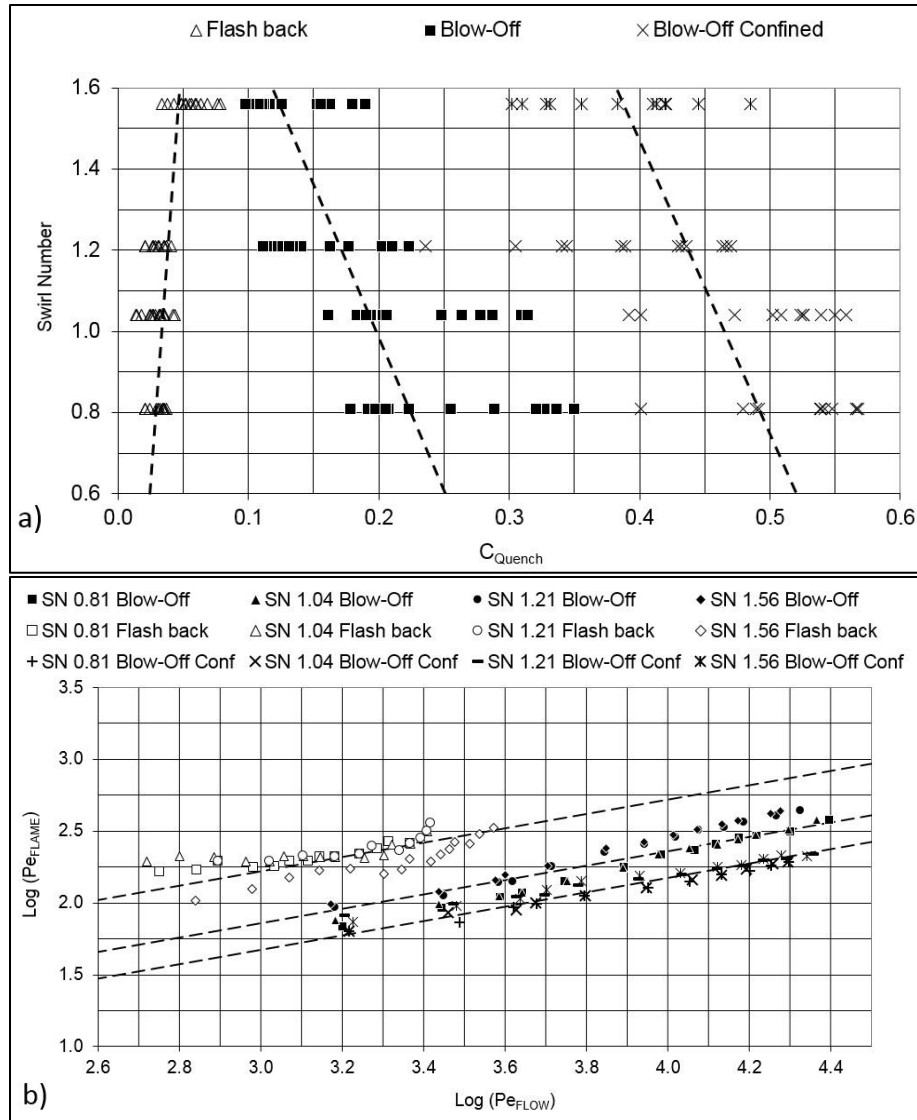
Fig. 12 – a) Methane Quench parameter; b) Methane Blow-off and Flashback Peclet correlations

The Peclet approach methodology which has been demonstrated for Methane can now be applied to the results obtained for practical steel industry waste gases. Fig. 13a shows the calculated quenching parameter and Fig 13b shows the Peclet relationship results for the COG data. The calculated quench parameter values for COG shown in Fig. 13a exhibit the same trends to those for methane, with there being evidence of a reduction in the calculated quench parameter for the blow-off conditions as swirl number is increased; and also no significant change in the calculated quench parameter values for changing swirl numbers for the flashback conditions. The calculated quench parameter for the COG flashback conditions are lower than that of the blow-off conditions for all of the swirl number values.

Again, average values for the quench parameter at the flashback and blow-off conditions were used to calculate y-intercept values for trend lines for the Peclet correlation graph (Fig. 13b). For COG the Peclet relationship shown in Fig. 13b shows that that the lean blow-off results follow the relationship defined by equation 10 for the range of results obtained with a good degree of correlation, albeit with greater variation compared to the methane data. At the higher flow conditions, corresponding to Reynolds numbers greater than the 4400 threshold previously identified, the flash back results for COG also follow the correlation. For the flashback results at the lower Reynolds number, corresponding to laminar flow conditions, the Peclet approach does not seem to apply. From this it can be determined than in order for the Peclet methodology to be used for the comparison of (and possibly prediction of) flame stability

13

conditions, the Reynolds number of the burner exit flow must be turbulent. An explanation for this is that the low Reynolds number flames seen at the low mass flow COG flashback conditions will exhibit a different flow structure to the higher Reynolds number turbulent flames, due to the absence of any acceleration in the flame speed caused increasing levels of turbulence.
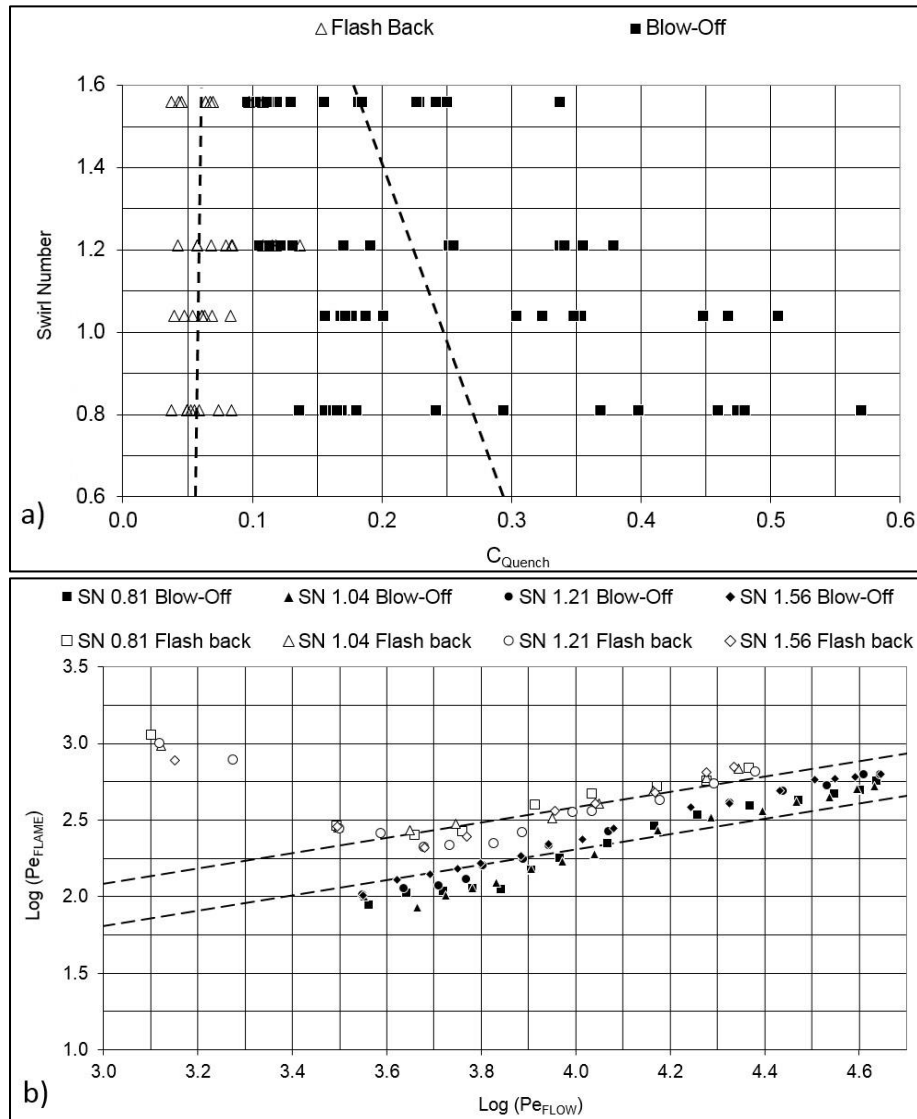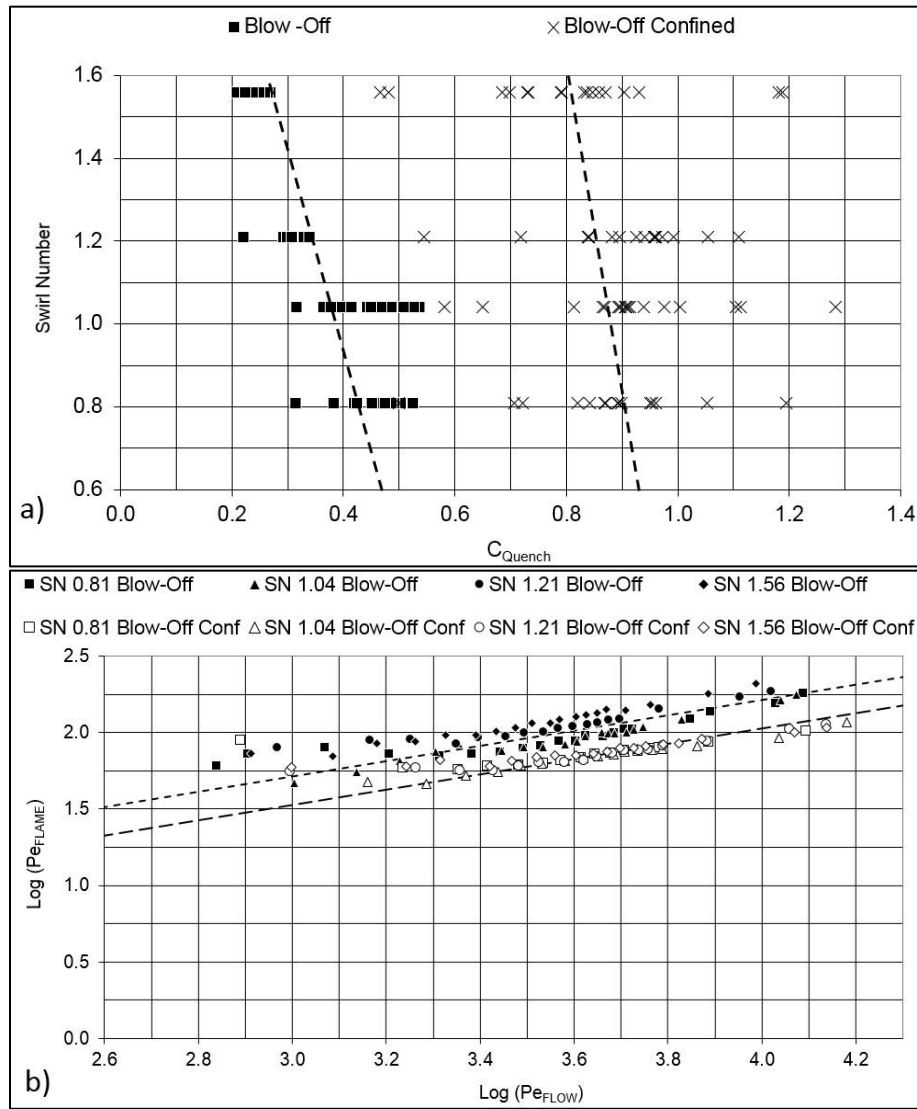

Fig. 13 - a) Calculated Coke Oven Gas Quench parameters; b) Coke Oven Gas Blow-off and flashback Peclet correlations

Fig. 14 shows the calculated quenching parameter values and the Peclet relationship for the BOS gas blow-off conditions, both with and without the use of confinement. For BOS gas it can be seen in Fig 14a that the calculated values of the quench parameter for the blow-off conditions (both with and without confinement) are seen to reduce as swirl number is increased. Like that seen in the methane data, the use of confinement increases the blow-off quench parameter values for BOS gas.

Dashed lines with y-intercepts calculated using the mean values for the quench parameter are shown in the Peclet correlation graph Fig. 14b. The BOS gas results again compare closely with the Peclet correlation for the higher flow conditions. Further work is required to explore the deviation that occurs at lower Pe_{FLOW} values, however it is suspected that this deviation coincides with the change in nature of the flow from turbulent to approaching laminar.

Comparing the BOS gas results to that of methane and COG it can be seen that the calculated values of the blow-off quench parameters are higher, which is most likely to be caused by the lower S_L of BOS gas, reducing the blow-off resistance.

Fig. 14 – a) Basic Oxygen Steelmaking gas Quench parameters; b) Basic Oxygen Steelmaking gas Blow-off and flash back Peclet correlations

Fig. 15 shows the calculated quenching parameter values and the Peclet relationship results for the blow-off conditions for BFG, both with and without the use of confinement. The quench parameter values for BFG shown in Fig 15a again follow the same trends as that seen with the other fuel gases; such as an increase in swirl number causing a decrease in the mean values obtained for the quench parameter. Again average values are used to produce y-intercept values of the dashed lines in the Peclet correlation graph Fig. 15b. The calculated values of the blow-off quench parameters for BFG are much higher than those of the other fuel gases presented, primarily due to the laminar burning velocity of BFG gas being significantly lower than that of the other fuels, and the flame more susceptible to blow-off. Again, a deviation from the trend line occurs at the lower Pe_{FLOW} values, which as previously mentioned is suspected to be due to the change in nature of the flow from turbulent to approaching laminar.
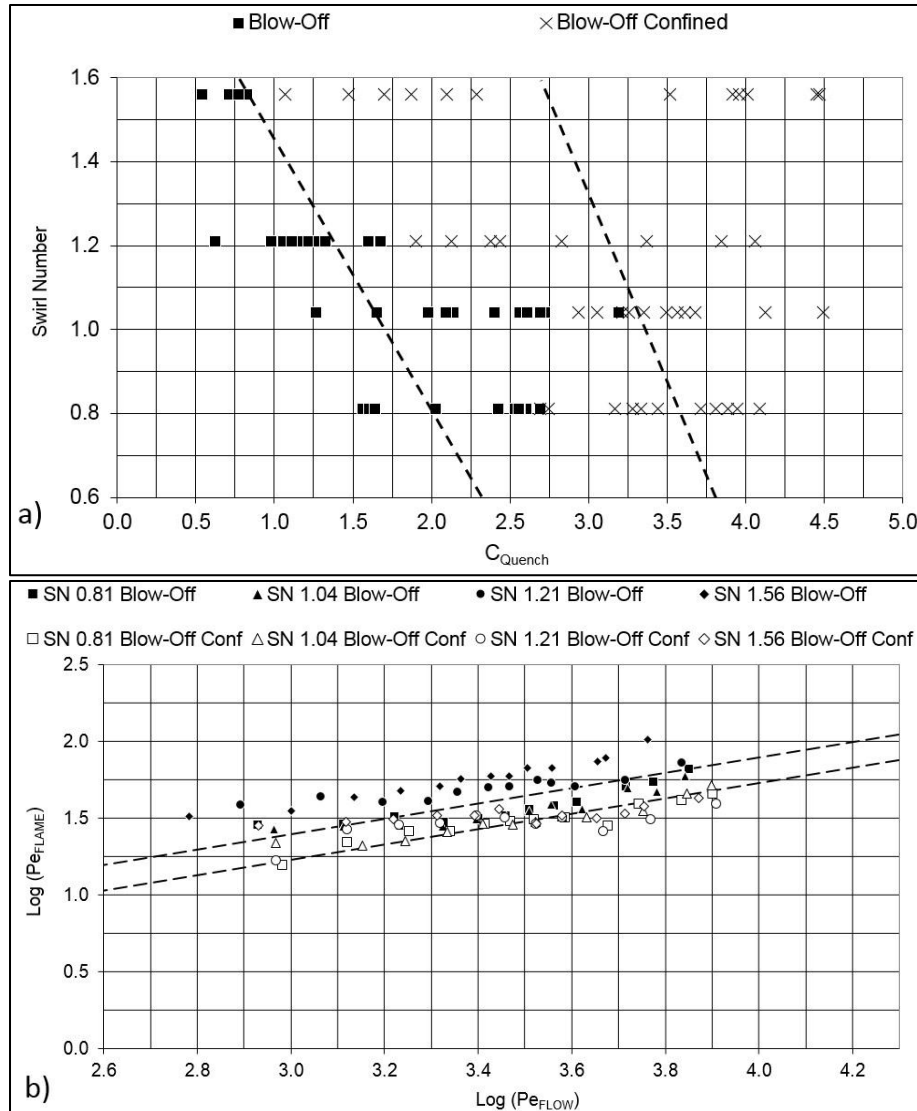
Fig. 15 – a) Blast Furnace Gas Quench parameters; b) Blast Furnace Gas Blow-off and flashback Peclet correlations

Previous work [14, 17 – 19] has shown that the Peclet number approach can be used in conjunction with a quench parameter to characterise the flash back and blow-off behaviour for burners. Kröner et al [14] suggest that there is a characteristic quench parameter that is constant for a particular burner configuration, whilst Dam et al [19] proposed that this quench parameter will not change despite changes in fuel composition. It can be seen that contrary to that proposed by Dam et al.[19], the quench factor does vary depending on the fuel used and is not dependent just on burner geometry. The observed quench factor is a measure of flash back resistance [14], and is seen in this work to reduce as fuel reactivity increases. The quench factor also reduces when the burner swirl number is increased.

To improve predictive capability of this relatively simplistic approach, accommodation of the flow characteristics and the interaction on flame chemistry need to be taken into consideration. However, the basic Peclet number approach allows for a comparison between fuels, swirl numbers and confined / unconfined conditions, and shows potential for use as a basic, first order, predictive tool for industrial applications. Further investigations into quantifying the effect of turbulence on values for Pe_{FLAME} may provide insight into developing the Peclet approach, such that results from small scale laboratory studies can be extrapolated towards developing burners for industrial applications.

16

5.   Conclusions

An experimental investigation of the behaviour of steelworks gases has been carried out using a variable swirl burner. Results have shown that there is a clear dependence of fuel composition on the flashback and blow off limits, which is further connected to the geometry and confinement used in the burner. It was found that:

- The different flame speeds of the gas mixtures used in the experiments (methane, COG, BOS gas and BFG) was shown to have a significant effect on the limits of the stable operating envelope that the swirl burner used could function. The high flame speed of COG resulted in flashback at flow conditions that would cause the other gas mixtures to blow-off.
- BOS gas was shown to have a very similar stable operating envelope to that of methane, while BFG was shown to have a much smaller stable operating envelope, blowing-off at lower flow rates for all equivalence ratios and burner configurations.
- The Peclet number parametric modelling approach has been successfully applied to represent stability limit data for methane and three steel industry process gases covering a range of reactivities and over a range of burner swirl configurations.
- Data for COG flashback stability limits were found to traverse the laminar / turbulent flow regimes, with the laminar results deviating from the Peclet correlation. This has not been reported previously.
- The quench factor (C_{Quench}) which has been previously applied in the Peclet correlation was shown to be dependent not only on the burner geometry, but also the properties of the fuel.

6.   Acknowledgements

References

1   JRC Reference Report, 2013, Best Available Techniques (BAT) Reference Document for Iron and Steel Production. European Commission.
2   Pugh DG, O'Doherty T, Griffiths AJ, Bowen PJ, Crayford AP, Marsh R (2013) Sensitivity to change in laminar burning velocity and Markstein length resulting from variable hydrogen fraction in blast furnace gas for changing ambient conditions, International Journal of Hydrogen Energy, 38 (8): 3459-3470.
3   Pugh D, Giles A, Hopkins A, O'Doherty T, Griffiths AJ, Marsh R (2013) Thermal distributive blast furnace gas characterisation, a steelworks case study, Applied Thermal Engineering, 53 (2): 358–365
4   Paubel X, Cessou A, Honore D, Vervisch L, Tsiava R (2007) A flame stability diagram for piloted non-premixed oxycombustion of low calorific residual gases, Proceedings of the Combustion Institute 31:3385-3392
5   Hou SS, Chen CH, Chang CY, Wu CW, Ou JJ, Lin TH (2011) Firing blast furnace gas without support fuel in steel mill boilers, Energy Conversion and Management, 52:2758-2767.
6   Subramanya M, Choudhuri A (2007) Investigation of combustion instability effects on the flame characteristics of fuel blends, in: 5th Int. Energy Convers. Eng. Conf. Exhib. Proc.
7   Thornton JD, Chorpening BT, Sidwell TG, Strakey PA, Huckaby ED, Benson KJ (2007) Flashback detection sensor for hydrogen augmented natural gas combustion, in: Proc. ASME Turbo Expo.
8   Syred N, Beer JM (1974) Combustion in swirling flow: a review, Combustion and Flame 23:143-201.
9   Lefebvre AH (1999), Gas Turbine Combustion, Taylor & Francis Group, New York
10 Valera-Medina A, Syred N, Griffiths AJ (2009) Visualization of isothermal large coherent structures in a swirl burner, Combustion and Flame 156:1723-1734
11 Valera-Medina A, Syred N, Bowen PJ, Crayford A (2011a) Studies of Swirl Burner Characteristics, Flame Lengths and Relative Pressure Amplitudes, Journal of Fluids Engineering 133 (10): 101302-101313
12 Valera-Medina A, Syred N, Kay P, Griffiths A, (2011b) Central Recirculation Zone Analysis in an Unconfined Tangential Swirl Burner with Varying Degrees of Premixing, Journal of Experiments in Fluids 50 (6):1611-1623
13 Plee SL, Mellor AM (1978) Review of flashback reported in prevaporizing/premixing combustors, Combustion and Flame 32:193-203

14   Kroner M, Fritz J, Sattelmayer T (2003) Flashback Limits for Combustion Induced Vortex Breakdown in a Swirl Burner, Journal of Engineering for Gas Turbines and Power, 125:693-700

15   Sheen HJ, Chen WJ, Jeng SY, Huang TL (1996) Correlation of Swirl Number for a Radial-Type Swirl Generator, Experimental Thermal and Fluid Science 12:444-451

16   Vigueras-Zuniga MO, Valera-Medina A, Syred N, (2012) Studies of the Precessing Vortex Core in Swirling Flows, Journal of Applied Research and Technology, 10 (5): 755-765.

17   Putnam AA, Jensen RA. (1949) Application of dimensionless numbers to flash-back and other combustion phenomena. Third symposium on combustion and flame and explosion phenomena. Baltimore: Williams and Wilkins. 89-98

18   Prade B, Lenze B (1992) Experimental investigation in extinction of turbulent non-premixed disk stabilized flames. Twenty-Fourth Symposium on Combustion, 369-375

19   Dam B, Corona G, Hayder M, Choudhuri A (2011) Effects of syngas composition on combustion induced vortex breakdown (CIVB) flashback in a swirl stabilized combustor, Fuel 90: 3274-3284

20   Syred N, Abdulsada M, Griffiths AJ, O'Doherty T, Bowen PJ (2012), The effect of hydrogen containing fuel blends upon flashback in Swirl Burners, Applied Energy 89:106-110

21   Abdulsada M, Syred N, Griffiths AJ, Bowen PJ (2011a) Effect of swirl number and fuel type upon the flashback in swirl combustors, paper AIAA-2011-0062 , 48th AIAA Aerospace Sciences meeting

22   Abdulsada M, Syred N, Griffiths AJ, Bowen PJ, Morris S (2011b) Effect of swirl number and fuel type upon the combustion limits in swirl combustors, ASME Turbo Expo, Canada.

23   Abdulsada M, Syred N, Bowen PJ, O'Doherty T, Griffiths AJ, Marsh R, Crayford A (2012) Effect of Exhaust Confinement and Fuel Type upon the Blowoff Limits and Fuel Switching Ability of Swirl Combustors, Applied Thermal Engineering, 48:426-435

24   Valera-Medina A, Syred N, Bowen P, 2013. (2013) Central recirculation zone visualization in confined swirl combustors for terrestrial energy, Journal AIAA Propulsion and Power 29 (1):195-204.

25   Stappert K (2003) Coriolis mass flow meters for natural gas measurement, Global Business Development Manager-Natural Gas Emerson Process Management-Micro Motion, Inc. 9906A 43rd St. Tulsa, Oklahoma

26   Bowman CT, Frenklach M, Gardiner WC, Smith GP (1999) The 'GRIMech 3.0' chemical kinetic mechanism. http://combustion.berkeley.edu/gri-mech/version30/text30.html

27   Li J, Zhao Z, Kazakov A, Chaos M, Dryer F.L (2007) A comprehensive kinetic mechanism for CO, CH2O, and CH3OH combustion. International Journal of Chemical Kinetics, 39:109–136.

28   Shelil N, Griffiths A, Bagdanavicius A, Bowen PJ, Syred N, Crayford AP (2010) Investigations of Gaseous Alternative Fuels at Atmospheric and Elevated Temperature and Pressure Conditions, ASME Turbo Expo, Glasgow

29   Wilke C. (1950) A viscosity equation for gas mixtures. The Journal of Chemical Physics 18 (4):517-519

30   Pugh DG, Crayford A, Bowen P, O'Doherty T, Marsh R, Steer J (2014) Laminar flame speed and Markstein length characterisation of steelworks gas blends, Applied Energy 136:1026-1034

31   Pugh DG, Crayford AP, Bowen PJ, Al-Naama M (2015) Parametric investigation of water loading on heavily carbonaceous syngases, Combustion and Flame, 164:126-136.

32   Lindsay A, Bromley L (1950) Thermal conductivity of gas mixtures, Industrial and Engineering Chemistry, 42 (8): 1509-1511

33   Kaviany M (2002) Principles of Heat Transfer, John Wiley & Sons, New York